

# SECONDARY ELECTRON EMISSION FROM SOLID SURFACES BOMBARDED BY MEDIUM ENERGY IONS

By E. R. CAWTHON\*

[Manuscript received 5 March 1971]

## *Abstract*

The results of Cawthon, Cotterell, and Oliphant for the emission of electrons produced by bombardment of a metal surface with various kinds of positive ions are compared with the predictions of proposed theories. It is seen that the complexity of the interaction processes occurring when a positive ion enters a surface is such that the emission process can only be described in a non-analytical manner, using a statistical treatment. The following discussion indicates that the observed results can be predicted qualitatively over a reasonable range of bombarding energies for many targets and ions by applying the theory of Parilis and Kishinevski. The energy loss cross sections, as well as the actual ionization cross sections, are shown to be important factors in determining the total emission.

## I. INTRODUCTION

When slow ions (ions with velocity less than the orbital velocities of the target electrons) interact with matter at not too low energies (i.e. ion energy  $\geq 100$  eV), appreciable interpenetration of the electron clouds occurs and many electrons of the atoms partake in the interaction. Lindhard and Scharff (1953, 1960) and Lindhard and Winther (1964) showed, using a statistical Thomas-Fermi model, that such an ion decelerates or loses energy by two distinct methods, namely elastic and inelastic processes, and they calculated the appropriate stopping cross sections  $S_n$  and  $S_e$ .

The expression

$$S_e = 25e^2 a_0 \frac{Z_1^{5/6} Z_2}{(Z_1^{2/3} + Z_2^{2/3})^{3/2}} \frac{v_0}{v_H}, \quad (1)$$

is sufficiently accurate provided

$$v_0/v_e \lesssim Z_1^{2/3}, \quad (2)$$

where  $v_0$  is the velocity of the incident ion and  $v_H$  is the Bohr orbital electron velocity. In expression (1),  $e$  is the electronic charge,  $a_0$  is the Bohr radius, and  $Z_1$  and  $Z_2$  are the atomic numbers of the incident ion and the target particle respectively. For protons, the condition (2) is

$$E_0 \lesssim 27 \text{ keV},$$

while for  $\text{Ar}^+$  ions

$$E_0 \lesssim 60\,000 \text{ keV}.$$

Thus, equation (1) has been used with confidence to help interpret the present experimental results. This equation predicts that at most velocities considered here

\* Research School of Physical Sciences, Australian National University, P.O. Box 4, Canberra, A.C.T. 2600; present address: P.O. Box 440, Manuka, A.C.T. 2603.

$S_e$  is proportional to the velocity, as might be expected from simple physical considerations. (At low velocities the energy loss would be proportional to velocity for an atom moving through an electron gas of constant density (Lindhard and Scharff 1953, 1960; Lindhard and Winther 1964; Datz 1968).) The quantity  $S_e$  then is the cross section for decelerating low energy ions (i.e. meeting the condition (2)) by interaction with free and quasi-free electrons in a solid. At higher velocities ( $v_0/v_e \gg Z_1$ ) the Bethe (1930) stopping formula must be used,  $S_e$  passing through a maximum at

$$v_0/v_e \sim Z_1^{2/3},$$

where  $v_e$  is a typical orbital electron velocity.

Several attempts have been made to explain kinetic secondary electron emission as the transfer of energy to free or quasi-free electrons. However, for intermediate energies (5–50 keV) the predominant process involves energy loss to lattice atoms or tightly bound inner electrons.

When two particles collide at not too low energies (i.e. energies say  $> 100$  eV) it has been noted that considerable interpenetration of the electron clouds occurs and many electrons of the atoms partake in the interaction—not merely the free or loosely bound electrons considered above. This is why a Thomas–Fermi type treatment is needed for a complete description. Unfortunately the Thomas–Fermi interaction potential is non-analytical, although it has been tabulated numerically by Gombas (1956). However, at sufficiently low velocities, such as those mostly covered in the present work, the Thomas–Fermi potential can be approximated by a simple Nielsen (1956)  $r^{-1}$ -type screening, leading to the expression

$$S_n = 3 \cdot 6 e^2 a_0 \frac{Z_1 Z_2}{(Z_1^{2/3} + Z_2^{2/3})^{1/2}} \frac{M_1}{M_1 + M_2}, \quad (3)$$

for the nuclear or elastic stopping cross section. Equation (3) is independent of velocity and is thus an approximation that is useful for qualitative discussions. The nuclear stopping cross section, as given by (3) is similar to that used by Bohr (1948) and, while the correct Thomas–Fermi function is more realistic, equation (3) lends itself to simple calculation and is a relatively good approximation at lower velocities.

From equations (1) and (3), we can construct the following tabulation for 10 keV ions on a platinum target.

| Incident Ion    | $S_n/S_e$ | $S_n/S_T$ (%) | $S_e/S_T$ (%) |
|-----------------|-----------|---------------|---------------|
| H <sup>+</sup>  | 0·021     | 2             | 98            |
| He <sup>+</sup> | 0·18      | 15            | 85            |
| N <sup>+</sup>  | 1·7       | 63            | 37            |
| Ar <sup>+</sup> | 8·1       | 89            | 11            |

For light ions we see that  $S_e$  exceeds  $S_n$  and so most energy will be lost by collisions with free or quasi-free (lightly bound) electrons between nuclear scattering events. Thus they would have relatively broad reflected spectra (Cawthron, Cotterell, and Oliphant 1969*b*). Heavier particles such as Ar<sup>+</sup>, however, would lose energy mainly through nuclear (elastic) processes near the surface and would have relatively sharp spectra (Cawthron, Cotterell, and Oliphant 1969*b*). It was seen in Cawthron, Cotterell,

and Oliphant (1969*b*) that most back-scattered particles are without charge, up to energies of several keV. In the present paper, discussion is confined to electron emission as ion scattering has been dealt with by Cawthron, Cotterell, and Oliphant (1969*b*, 1970).

## II. EXPERIMENTAL RESULTS

The secondary emission coefficient  $\gamma$  is defined as the average number of electrons released from a solid per incident particle under particle bombardment. The method of measurement has been fully described by Cawthron, Cotterell, and Oliphant

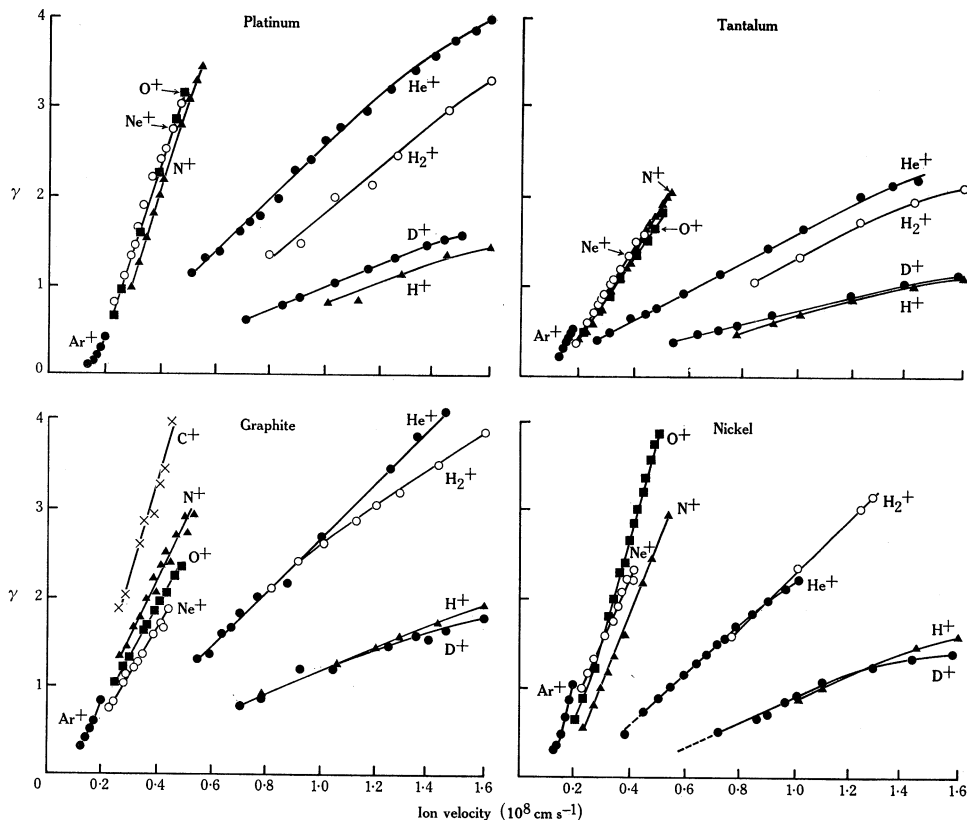


Fig. 1.—Variation of the secondary electron emission coefficient  $\gamma$  with the velocity of the incident ion for platinum, tantalum, graphite, and nickel targets.

(1969*a*) and is not reiterated in detail here. Briefly, it involved the use of a magnetic field to channel the electrons into a Faraday cup, where they were measured independently of any scattered or sputtered ions. The target was red hot in all cases and was inclined  $45^\circ$  to the incident beam. The pressure in the collision chamber under working conditions was 20–40 ntorr and the target was flashed at considerably higher temperature, depending upon the material, until reproducible results were obtained and until there was no apparent temperature coefficient for electron emission. In this paper the experimental results for  $\gamma$  are plotted as functions of beam velocity, for the

purposes of the present discussion. Also, velocity is a more fundamental variable and more convenient than energy from the point of view of theoretical discussion.

(1) Figure 1 shows that the variation with velocity is linear from ion velocities very close to threshold (for  $\text{Ar}^+$  ions) to velocities an order of magnitude greater for platinum, tantalum, graphite, and nickel targets. Departure from linearity occurs at both the lowest velocities investigated ( $\sim 10^7 \text{ cm s}^{-1}$  for argon) and the highest velocities ( $\sim 1.2 \times 10^8 \text{ cm s}^{-1}$  for protons). At velocities very near threshold the dependence apparently becomes of the form  $v^2$ , while at sufficiently high velocities the emission starts to saturate.

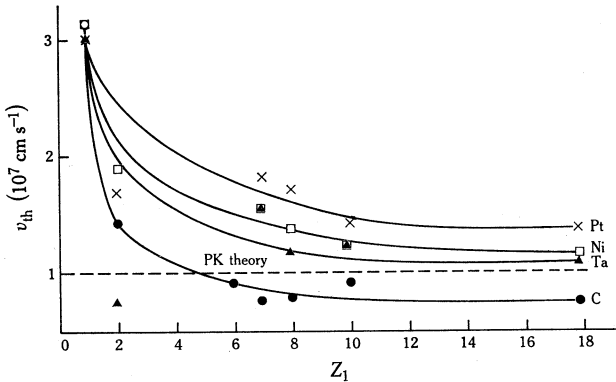


Fig. 2.—Variation of the extrapolated thresholds  $v_{th}$  for kinetic emission with the atomic number  $Z_1$  of the incident ion for four targets.

(2) The threshold for kinetic emission may be estimated approximately by extrapolating the linear portions of the emission-velocity variation back to the velocity axis in Figure 1. The extrapolated thresholds are plotted in Figure 2 as a function of  $Z_1$  for four targets. It can be seen that the thresholds tend to be high for light ions and to remain constant for heavier targets at a velocity in the vicinity of  $10^7 \text{ cm s}^{-1}$ . This difference in behaviour between heavy and light ions is not surprising in view of the discussion in Cawthron, Cotterell, and Oliphant (1969*a*), and a theory which explains the behaviour over the entire  $Z_1$  range would have to take into account both elastic and inelastic energy loss processes for light ions.

(3) The quantity  $\gamma$  cannot be directly identified with the secondary electron emission  $\gamma_{kin}$  for kinetic emission, owing to the presence of potential emission which makes a contribution  $\gamma_{pot}$  so that

$$\gamma = \gamma_{kin} + \gamma_{pot}. \quad (4)$$

This is considered further in Section III(*a*), but it is noted here that the extrapolated thresholds for  $\text{He}^+$  ions on tantalum and platinum targets in Figure 2 are lower than might be expected because of a higher potential contribution.

(4) The dependence of  $\gamma$  on the nuclear charges of the target particles is difficult to determine quantitatively. As might be expected, at a given velocity above threshold the atomic numbers of the incident and target particles, not the mass numbers, are the important parameters in determining the total emission, the potential being of the screened-Coulomb type (Lindhard and Scharff 1953, 1960; Lindhard 1954; Lindhard and Winther 1964; Datz 1968). The results indicate that the emission

coefficient is roughly proportional to  $Z_1$ , and indeed we can formulate the empirical relation

$$\gamma = \{(v - v_{th})/X\}Z_1, \tag{5}$$

where  $v_{th}$  is the extrapolated threshold,  $v (\equiv v_0)$  is the incident ion velocity, and  $X$  is some function of  $Z_2$ . It has not been possible to relate this  $X$  factor to any specific physical property of the target; it is  $\sim 2$  for platinum and carbon,  $\sim 2.5$  for nickel, and  $\sim 4$  for tantalum. While tantalum gives a lower emission for a given incident ion at a given velocity above threshold than any other target, there is no directly apparent relationship between  $\gamma$  and  $Z_2$ .

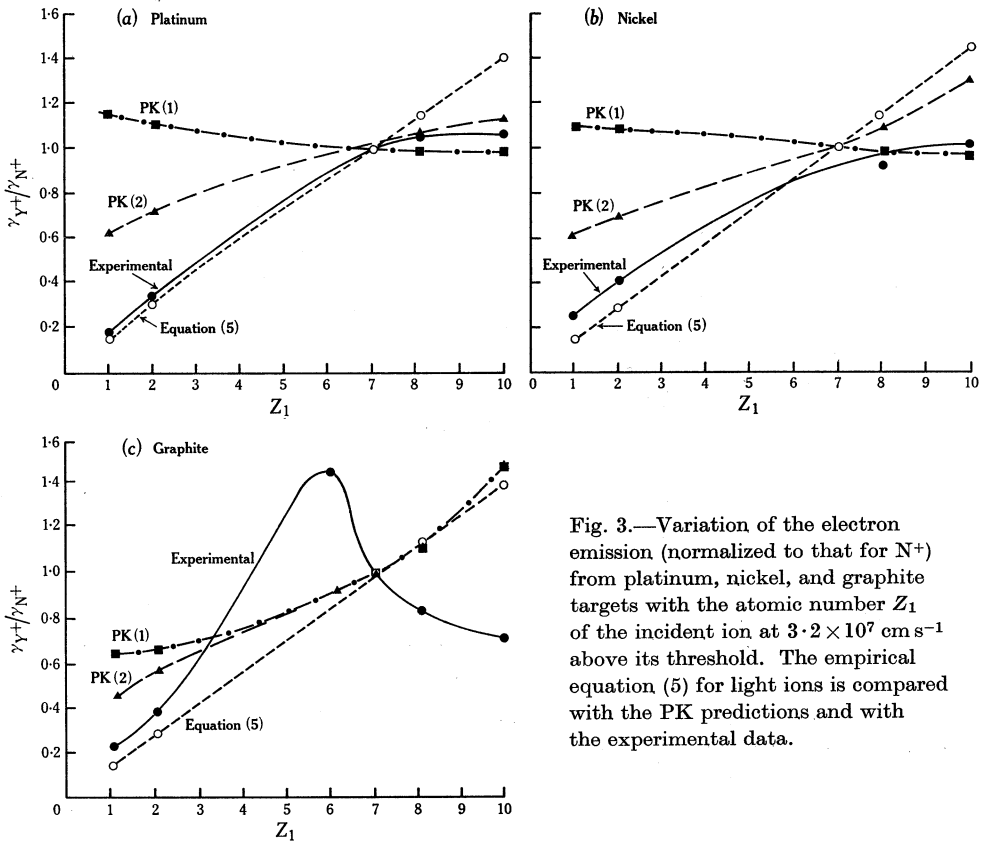


Fig. 3.—Variation of the electron emission (normalized to that for  $N^+$ ) from platinum, nickel, and graphite targets with the atomic number  $Z_1$  of the incident ion at  $3.2 \times 10^7 \text{ cm s}^{-1}$  above its threshold. The empirical equation (5) for light ions is compared with the PK predictions and with the experimental data.

In Figures 3(a) and 3(b), the expression (5) is compared with the theoretical predictions of the theory of Parilis and Kishinevski (1960, 1963) for both light and heavy ions and also with the experimentally observed data for platinum and nickel targets. The data are normalized to the observed emission for  $N^+$ . The Parilis and Kishinevski (PK) theory is discussed in more detail in Section III(b), but it can be seen that it is not very accurate for light ions ( $S_e > S_n$ ) and when  $Z_2 \gg Z_1$  ( $Z_1 = 1, 2, \text{ or } 3$ )

$$S_e = 25e^2a_0Z_1v_0/v_H. \tag{6}$$

We might thus expect some dependence such as (5), or at least expect  $\gamma$  to vary closely linearly with  $Z_1$  for light ions. The dependence on  $Z_2$  is not so clear, as both quantities must enter into a detailed discussion of the energy loss and electron emission processes. The PK theory is much more accurate when  $S_n \gg S_e$ , that is, for the heavier bombarding particles.

Figure 3(c) shows the results for a graphite target and it is interesting in that none of the proposed equations is satisfactory for the heavier bombarding ions, and the experimental data indicate a peak in the emission for carbon ions on a graphite target, with the emission actually decreasing for heavier ions. The peak occurs for  $Z_1 = Z_2 = 6$  and the presence of some surface effect, leading to enhanced apparent emission for carbon ions on graphite, cannot be ruled out (see Section III(b)).

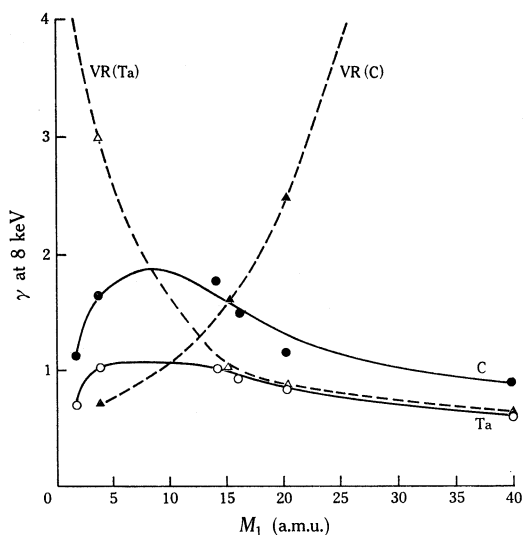


Fig. 4.—Results for the variation of the electron emission with the mass  $M_1$  of the incident ion at 8 keV ion energy compared with the predictions (normalized) of the Von Roos (VR) theory for graphite and tantalum targets.

(5) Figure 4 plots the emission coefficient  $\gamma$  at a beam energy of 8 keV against the incident ion mass for two targets, graphite and tantalum. Omitting the results for protons, it can be seen that  $\gamma$  increases with  $Z_1$  initially, peaking at several a.m.u. The emission then drops until, for incident  $\text{Ar}^+$ , it has fallen to a value close to that for deuterium ions again. The data are presented in this form as it enables us to check the prediction of Von Roos (1957) that

$$\gamma \propto (1 + \mu)^4 / \mu \quad (7)$$

at constant incident ion energy, where

$$\mu = M_1 / M_2.$$

The theory of Von Roos is discussed in more detail in Section III(c). The predictions of the Von Roos theory are drawn to be coincident with the experimentally observed plots at 15 a.m.u. incident ion mass. Experimental data for platinum and nickel targets are not included as they follow the same trends as for tantalum. Graphite is used as representative of a target of low  $Z_2$  value. The Von Roos theory, like the

PK theory, falls down for light ions on heavy targets and fails completely for a light target, irrespective of ion mass.

(6) The experimental results indicate no dependence of  $\gamma$  upon the ionic charge. Only singly charged ions have been used for the above work but, at a given velocity above threshold and for a given target and ion species,  $Z_1$  is the principal factor affecting the emission. This is discussed in more detail by Cawthron, Cotterell, and Oliphant (1969*a*) where the emission is plotted as a function of incident ion energy, rather than velocity.

### III. DISCUSSION

#### (a) *Potential Contribution to Emission*

This paper is primarily concerned with kinetic ejection but a consideration of potential emission is necessary to explain certain aspects of the experimental data. As has already been noted, the measured quantity  $\gamma$  contains a contribution arising from the potential emission of electrons. Potential emission involves the transfer of potential energy from the incident ion to a conduction band electron, leading to emission by processes explained by Hagstrum (1955, 1956). For ion-target systems where the ionization energy exceeds twice the work function, there will always be a potential contribution to the total emission, and this contribution will be nearly independent of the kinetic contribution  $\gamma_{\text{kin}}$ . The contribution  $\gamma_{\text{pot}}$  becomes especially significant for ions with high ionization potential. Upon the basis of kinetic emission alone, we would expect  $\gamma = 0$  at extremely low bombarding velocities. However, Hagstrum (1955, 1956) showed that  $\gamma$  was about 0.25 for He<sup>+</sup> ions on a molybdenum target, at bombarding velocities close to zero, and that  $\gamma$  retains this value up to the threshold for kinetic emission. There is nothing to suggest that potential emission does not extend up to much higher velocities such as those employed in the present experiments.

For hydrogen, deuterium, nitrogen, and oxygen ions on the present targets, the potential contribution is very small and  $\gamma \approx \gamma_{\text{kin}}$ . However, for helium, neon, and argon ions, particularly the former two,  $\gamma_{\text{pot}}$  certainly cannot be ignored. In Figure 2, potential emission probably accounts for the thresholds for helium ions on platinum and tantalum and, to a much lesser extent, nickel, being lower than expected for deuterium ions. There is no irregularity in the emission for a graphite target, only a steady decrease in  $v_{\text{th}}$  with  $Z_1$ . In Figure 1, there are also marked (but constant) differences in the emission between He<sup>+</sup> and H<sub>2</sub><sup>+</sup> for platinum and tantalum, but very little difference for graphite and nickel targets (for velocities  $\lesssim 1.0 \times 10^8$  cm s<sup>-1</sup>).

In Figure 1, it is difficult to explain the non-coincidence of the emission curves for H<sup>+</sup> and D<sup>+</sup> on a platinum target, as they have the same  $Z_1$  value and presumably much the same thresholds. Possibly there was systematic error in measuring the emission from one of these particular ions in the case of platinum. For tantalum, graphite, and nickel targets, the results for H<sup>+</sup> and D<sup>+</sup> are the same within the experimental error, for velocities  $\lesssim 1.2 \times 10^8$  cm s<sup>-1</sup>. The energy loss process is mainly due to electronic (inelastic) collisions for the light ions and only the nuclear charges, not the masses, enter into the expression for  $S_e$  (equation (1)). However, there could be some abnormality arising from the mobility of hydrogen in hot

platinum which may be highly dependent upon the target temperature and the mass of the incident ion.

All the theories discussed below assume a homogeneous non-crystalline target and hence take no account of the effects of channelling. Thus they cannot be taken very seriously in the strict quantitative sense.

(b) *PK Theory*

One of the most successful theories for explaining kinetic emission in a qualitative sense is that of Parilis and Kishinevski (1960, 1963). They assumed  $S_n > S_e$  and that the energy transfer occurs to excited states along the statistical lines discussed by Firsov (1959). The so-called "heating" of the electronic clouds was assumed to occur by virtue of their assimilation of the translational motion of the nuclei. This assumption enabled them to calculate the energy  $\delta E$  transferred to the bound electrons which was necessary to raise them across the forbidden band. They assumed the excitation to be of the Auger type rather than direct excitation. The mathematics of their treatment will not be reiterated here, but their main concepts and results are discussed for comparison with experimental data, remembering that only qualitative and not quantitative agreement can be expected.

Parilis and Kishinevski (1960, 1963) expressed  $\gamma_{\text{kin}}(v)$  in the form

$$\gamma_{\text{kin}}(v) = N\sigma^*(v)\lambda\omega, \quad (8)$$

where  $N$  is the number of lattice atoms per  $\text{cm}^3$ ,  $\lambda$  is the mean free path for the electrons in the target,  $\sigma^*(v)$  is the effective ionization cross section for ionization of a lattice atom by the incident ion at velocity  $v$ , and  $\omega$  is the probability of the Auger electron process proceeding, i.e. of the excited electron escaping from the target. The probability  $\omega$  can be approximated by the empirical formula

$$\omega = 0.016(\delta - 2\phi), \quad (9)$$

where  $\delta$  is the hole depth and  $\phi$  the work function.  $\sigma^*(v)$  was not simply taken to be the cross section for ionization of a lattice atom by the incident ion, as  $S_n$  and  $S_e$ , the nuclear and electronic stopping cross sections, must be taken into account. For heavy ions,  $S_e$  is very much less than  $S_n$  and the energy loss per unit depth of penetration, for a given ion, occurs mainly through nuclear collisions, i.e. it is independent of velocity (equation (3)). Parilis and Kishinevski wrote

$$\sigma^*(v) = \sigma(v) - \Delta\sigma(v), \quad (10)$$

where  $\Delta\sigma$  accounts for the retardation of the ionization process with depth. This factor is given explicitly by Parilis and Kishinevski, who took the decrease in velocity with depth  $x$  to follow the simple law

$$v^2 - v_x^2 = kx, \quad (11)$$

where  $k$  is a constant and  $v_x$  the velocity at depth  $x$ ; this assumes that the energy loss per unit penetration is constant, i.e. that  $S_n \gg S_e$ . From the tabulation of cross sections in Section I we see that at medium energies this assumption is only true for

the heavier ions and we would not expect the theory to be valid for light ions, even in a qualitative sense, unless the expression (10) were modified to account for losses due to collisions with free or quasi-bound electrons. For heavy ions at medium energies, however, the theory is in reasonable qualitative agreement with experimental data (see Fig. 3). Parilis and Kishinevski, indeed, did rather arbitrarily restrict the validity of their theory to

$$\frac{1}{4} < Z_1/Z_2 < 4. \quad (12)$$

The ion will continue to produce electrons until, at some depth  $x = x_s$ , it undergoes a screened-Coulomb scattering process. At low velocities, for heavy ions, the  $v_x^2$  term in (11) becomes appreciable compared with  $v^2$ , the squared incident velocity, and so also the  $\Delta\sigma(v)$  factor in equation (10) becomes significant. Also, at sufficiently low velocities most back-scattered particles will emerge in the uncharged state (Cawthron, Cotterell, and Oliphant 1969*b*) as the incident ion will have a high probability of capturing an electron from the media. At much higher velocities the energy loss by the ion penetrating to a depth  $x_s$  is small, relative to the incident energy, and so the energy loss processes are of much less significance in calculating the total cross section for the emission process. We can now enumerate the main trends predicted by the above theory and compare them qualitatively with the present experimental data.

At very low velocities the ionization cross section will be too small for ejection of an electron by impact ionization and any emission occurring must be via the potential process. As usually the latter is quite small, the absence of kinetic ejection accounts for the experimentally observed thresholds. These are estimated by extrapolation in Figure 2 and for heavier bombarding ions  $v_{th}$  is not too different from the value

$$v_{th} = 1.05 \times 10^7 \text{ cm s}^{-1}$$

predicted by the PK theory for all target-ion combinations.

At velocities slightly above threshold the  $\Delta\sigma(v)$  factor in equation (10) becomes significant and the theory predicts

$$\gamma_{kin} \propto v^2 - \left(\frac{3}{2}v_{th}\right)^2, \quad (13)$$

that is, there is a  $v^2$  dependence for the emission. From Figure 1 the data are insufficient to determine the precise quadratic form, but the departure from linearity for the heaviest ion (Ar<sup>+</sup>) near threshold approximates a  $v^2$  dependence.

At velocities greater than  $2v_{th}$ , the PK theory predicts

$$\gamma_{kin} \rightarrow v \tan^{-1}\{0.6 \times 10^{-7}(v - v_{th})\} \rightarrow c(v - v_{th}), \quad (14)$$

where  $c$  is a constant, that is, the theory approaches a linear dependence, the velocity being measured above the threshold for kinetic ejection. This agrees with the experimental data for all ions, from velocities slightly above threshold to velocities of the order of  $1.2 \times 10^8 \text{ cm s}^{-1}$  for the lighter ions.

At higher velocities the electrons formed in the deeper layers cannot escape and the theory assumed an electron absorption probability function of the form  $\exp(-x/\lambda)$  in calculating the emission. For ions at the higher velocities (exceeding  $\sim 1.2 \times 10^8$

cm s<sup>-1</sup> in Fig. 1), saturation starts to occur because the average penetration depth  $x_s$  is sufficient to prevent an appreciable number of electrons escaping from the target. At even higher velocities the numbers reaching the surface are further decreased, so that  $\gamma$  starts to decrease and high energy theories such as that of Sternglass (1957) must be employed. However, the maximum occurs at velocities well above those attained in the present work. Thus we can consider  $S_e$  to be small relative to  $S_n$  for all except the lightest ions.

The PK theory predicts a mass dependence for the emission of the form

$$\{(Z_1 + Z_2)/(Z_1^{\frac{1}{2}} + Z_2^{\frac{1}{2}})\}^2$$

for heavy ions, and the slightly modified form

$$(Z_1^{\frac{1}{2}} + Z_2^{\frac{1}{2}})(Z_1^{\frac{1}{2}} + Z_2^{\frac{1}{2}})^3$$

for light ions, where electronic energy losses are more important. The above expressions will be referred to as PK(1) and PK(2) respectively. Figures 3(a) and 3(b) compare the predictions of the theory with the experimental measurements and with the empirical expression (5). As the present discussion confirms, the PK theory fails badly for light ions, even in its slightly modified form. Both PK(1) and PK(2) predict the correct trends for heavier ions (both expressions approach  $Z_2$ , a constant for a given target, if  $Z_2 \gg Z_1$ ). The normalized emission should thus approach unity approximately, as is observed for both PK(1) and PK(2), and for the experimental results.

For the case of a graphite target (Fig. 3(c)) no current theory can explain the normalized emission, especially the peak at  $Z_1 = Z_2 = 6$  and the decrease with  $Z_1 > 6$ . The PK theory fails even though the condition (12) is satisfied as for, say, N<sup>+</sup> on graphite ( $Z_1/Z_2 = 7/6$ ). However, graphite has a rather strange lamina structure and this may account for the irregularities in the experimentally observed emission.

The PK theory is one of the most successful in explaining the observed data, although it fails badly for light ions. It would seem that kinetic electron ejection is a consequence of the release of bound electrons by impact-ionization.

### (c) Other Theories

Von Roos (1957) assumed that the lattice atoms behave as a gas and that the incident ions have a distribution function influenced solely by elastic collisions between them and "free" lattice atoms. From the tabulation of cross sections in Section I it is evident that for light ions at medium energies, inelastic collisions with free or quasi-free electrons will mainly determine the distribution function, even if we accept his dubious assumption of a "gas" of lattice atoms which behaves like a classical gas. Von Roos also assumed that all secondary electrons formed actually escape from the metal, i.e. that the collision depth  $x_s$  is so small that the absorption factor  $\exp(-x_s/\lambda)$  is negligible. These considerations limit his theory to very low velocities and targets of high atomic number.

In Figure 4 the Von Roos (1957) prediction (equation (7)), like the PK theory, gives very close to the correct dependence of emission on the particle masses for

heavy ions on high  $Z_2$  targets. However, it does not predict the observed trends for a graphite (low  $Z_2$ ) target over any part of the incident mass range.

The theory of Izmailov (1960*a*, 1960*b*, 1962) assumes that kinetic ejection results from the transfer of energy to free (i.e. conduction-band) electrons by simple two-body collisions. However, Cawthron, Cotterell, and Oliphant (1969*a*) have shown that considerable numbers of secondary electrons are emitted with energies well above the maximum expected for simple two-body collisions. The theory of Izmailov predicts  $\gamma \propto v^2$  at low energies, which agrees with the prediction of the PK theory for velocities very close to threshold; however, its predictions are invalid for all higher velocities. The basic premises of the theory are clearly inadequate to explain the observed data and any agreement with experiment may be fortuitous.

#### IV. CONCLUSIONS

The experimental data of Cawthron, Cotterell, and Oliphant (1969*a*) indicate that kinetic electron ejection at medium energies arises from the ionization of lattice atoms by the incident particles. For the lighter ions (with  $Z_1$  values of 1, 2, ...), the main energy loss processes involve inelastic interactions with free or loosely bound electrons rather than with the nuclei of the target or with the inner bound electrons of the target. For most ions at medium energy, the mutual penetration of the electron clouds is appreciable and many electrons will take part in the interaction. The most successful theory to date seems to be that of Parilis and Kishinevski (1960, 1963). In the author's opinion, an elaboration of this theory to account for all sources of energy loss would give a fuller and more comprehensive understanding of the emission process.

#### V. REFERENCES

- BETHE, H. A. (1930).—*Annln Phys.* **5**, 325.  
 BOHR, N. (1948).—*Math.-fys. Meddr* **18**, 8.  
 CAWTHON, E. R., COTTERELL, D. L., and OLIPHANT, SIR MARK (1969*a*).—*Proc. R. Soc. A* **314**, 39.  
 CAWTHON, E. R., COTTERELL, D. L., and OLIPHANT, SIR MARK (1969*b*).—*Proc. R. Soc. A* **314**, 53.  
 CAWTHON, E. R., COTTERELL, D. L., and OLIPHANT, SIR MARK (1970).—*Proc. R. Soc. A* **319**, 435.  
 DATZ, E. (1968).—In "Methods of Experimental Physics". Vol. 7B. (Ed. B. Bederson.) (Academic Press: New York.)  
 FIRSOV, O. B. (1959).—*Soviet Phys. JETP* **9**, 1076.  
 GOMBAS, P. (1956).—In "Handbuch der Physik". (Ed. S. Flügge.) Vol. 36, pp. 109–231. (Springer-Verlag: Berlin.)  
 HAGSTRUM, H. D. (1955).—*Phys. Rev.* **104**, 317.  
 HAGSTRUM, H. D. (1956).—*Phys. Rev.* **104**, 672.  
 IZMAILOV, S. V. (1960*a*).—*Soviet Phys. solid St.* **1**, 1415.  
 IZMAILOV, S. V. (1960*b*).—*Soviet Phys. solid St.* **1**, 1425.  
 IZMAILOV, S. V. (1962).—*Soviet Phys. solid St.* **3**, 2046.  
 LINDHARD, J. (1954).—*Math.-fys. Meddr* **28**, 8.  
 LINDHARD, J., and SCHARFF, M. (1953).—*Math.-fys. Meddr* **27**, 15.  
 LINDHARD, J., and SCHARFF, M. (1960).—*Phys. Rev.* **124**, 128.  
 LINDHARD, J., and WINTHER, A. (1964).—*Math.-fys. Meddr* **34**, 3.  
 NIELSEN, K. (1956).—"Electromagnetically Enriched Isotopes and Mass Spectrometry." p. 63. (Butterworths: London.)  
 PARILIS, E. S., and KISHINEVSKI, L. M. (1960).—*Soviet Phys. solid St.* **3**, 885.  
 PARILIS, E. S., and KISHINEVSKI, L. M. (1963).—*Bull. Acad. Sci. USSR phys. Ser.* **26**, 1422.  
 STERNGLASS, E. J. (1957).—*Phys. Rev.* **108**, 1.  
 VON ROOS, O. (1957).—*Z. Phys.* **147**, 210.

